Hindawi
Advances in Materials Science and Engineering
Volume 2022, Article ID 7874016, 13 pages
https://doi.org/10.1155/2022/7874016

Research Article

Evaluation of Rock Burst Propensity and Rock Burst Mechanism in Deep Phosphate Mines: A Case Study of Sujiapo Phosphate Mine, Hubei Province, China

Qinrong Kang,[1] Yuandi Xia,[1] Minghan Shi,[2] Weizhong Zhang,[1] Weiqing Wang,[1] Dehua Kong,[1] and Yunpeng Wang[1]

[1]*School of Resources and Safety Engineering, Wuhan Institute of Technology, Wuhan 430073, China*
[2]*Hubei Yihua Group Mining Co., Ltd., Yichang, Hubei 443000, China*

Correspondence should be addressed to Weizhong Zhang; wzzhang1120@126.com

Received 30 October 2022; Revised 30 November 2022; Accepted 2 December 2022; Published 22 December 2022

Academic Editor: Dimitrios E. Manolakos

Rockburst is one of the major problems in rock underground engineering and mechanics. To make a risk assessment of rockburst and improve the mine safety index, some evaluation systems for rockburst propensity have been proposed and applied, and progress has been made in the study of high-value mines and single evaluation systems, but these evaluation systems are still immature for deep low and medium grade phosphate mines with more complex influencing factors. Therefore, to solve this problem, this study takes the phosphate mining area of the Sujiapo phosphate mine as the main research object, and combines the characteristics of the deep rockburst of the phosphate mine and its physical and mechanical properties; the evaluation system combines fuzzy mathematical method and multiple evaluation methods to determine the propensity of rockburst of deep mining of Sujiapo phosphate mine. The JSM-500LV SEM and acoustic emission results are used to analyze the microscopic mechanism of rockburst from the morphology and composition of the rocks, and the rationality of the evaluation system is further demonstrated. The study shows that dolomite and phosphorite in the study area are moderate rockburst, and shale has a weak rockburst tendency; because the roof dolomite and phosphorite crystallization degree are higher, the elastic modulus is large. Under the action of external load, the roof dolomite stored more elastic strain energy. Deformation damage consumes less energy. The energy released to the outside world after the damage is large, more likely to occur brittle damage, and the rockburst tendency is high. Therefore, the evaluation system combining multiple evaluation methods can comprehensively determine rockburst in phosphate mines.

1. Introduction

Phosphate resources have a strategic position in agriculture and industrial production, and with the continuous exploitation of phosphate resources, phosphate mining gradually develops to the deep. Due to the increase in the depth of burial of the rock, the more obvious the change in the surrounding pressure by underground excavation disturbance damage, the initial stress equilibrium state of the surrounding rock is broken [1], and the internal energy of the rock body is increasing, when the internal storage of elastic strain energy reaches a critical state suddenly released, the rock body occurred obviously brittle damage, or even ejection phenomenon, the phenomenon is known as rockburst [2]. Rockburst not only has sudden, violent, and other characteristics, in the deeply buried underground works also level easy to become a production disadvantage, threatening the safety of life [3–5].

Given the impact of rockburst, domestic and foreign scholars combined a large number of engineering examples of rock bursts to summarize the influencing factors, for example, Cai et al. [6] studied the high-stress energy accumulation environment of the rock was a necessary condition for rockburst, rockburst was prone to occur in intact

brittle rock, and rock lithology; the study by Zubelewicz and Mroz [7] found that the stress environment was one of the fundamental factors of rockburst, the plumb stress δ_V of the rock with depth roughly by the rock weight of the ratio of linear increase, that is, the deeper the burial depth, the more obvious rockburst; underground rock excavation disturbance, is prone to cause stress redistribution within the rock, and this redistribution of stress gradually decreases with the continuous advance of excavation. In recent years, more and more scholars have devoted themselves to the study of the rockburst mechanism. For example, Li et al. [8] took the Sichuan Baijiao coal mine as the research object and found that the fractal dimension of rockburst cracks was closely related to the stress transformation process occurring in rockburst. Lin et al. [9], with the help of electron microscopy scanning of the damaged surface of the specimen for fine morphological characterization, concluded that the mechanism of rock damage under different stress gradients is different.

With the depth of research, to quantitatively analyze the grade of rockburst, scholars from various countries have proposed a variety of discriminatory methods, but they were broadly grouped into two categories: theoretical analysis method and field measurement method [10, 11]. Theoretical analysis methods include (1) stress criterion method: Turchaninov criterion, Hoek criterion, Barton criterion, etc.; (2) lithological criterion: rock integrity evaluation, brittleness coefficient method (B value method), Gu Mingcheng criterion, etc.; (3) energy criterion method: strain energy storage indicators (W_{et}), impact energy indicators (W_{CF}), etc.; (4) critical depth criterion: Hou Faliang criterion, Pan Yishan criterion. Field actual measurement methods include acoustic emission tests, infrared thermal images, microgravity methods, etc. The application of numerical software, such as FLAC3D, PFC, and Abaqus finite element software was also widely used in the numerical simulation of rock explosions. And methods such as fuzzy mathematics [12], artificial neural networks [13], grey correlation theory [14], and particle swarm algorithms [15] can also be used to comprehensively process engineering values [16].

The current status of research on rockburst propensity and influencing factors shows that the analytical research on rockburst is mainly focused on high-value mines and single evaluation system research, and there is less research on rockburst propensity and mechanism for deep medium and low-grade phosphate mines. In this study, the rockburst propensity of the roof and floor of this deep-mining phosphate mine was determined based on indoor experimental results combined with various criterion methods, mainly using a deep medium and low-grade phosphate mine as the research object. In addition, combined SEM, acoustic emission three-dimensional imaging, and EDS mapping to analyze the damage and destabilization mechanism of the roof and floor ore rocks, and to investigate the mechanism of rockburst in the phosphate layer. This study combines previous methods to obtain comprehensive determination results. It can improve the accuracy of the results and contributes to the enrichment of rockburst studies of medium and low-grade phosphate mines.

2. Geological Overview and Rockburst Characteristics

2.1. Geological Overview of the Mine Site. Sujiapo phosphate mine is located in the town of Hehua, Yuan'an County, Yichang City, Hubei Province (see Figure 1(a)), geographical location 111°18′15″E~111°19′31″E, 31°14′34″N~31°16′09″N. The phosphate mine is a gently inclined thin ore body, a monoclinic structure, stratigraphic direction north-south, inclined east, the main industrial ore body ph_1^3 phosphate ore layer average dip is about 10°, the average thickness of the ore body is 2.71 m, and the burial depth is between +300 m and +950 m. There are no large fracture structures in the mine area, only a few small faults, and local folds and fissures are more developed. The roof of the mine is siliceous dolomite with good integrity, the floor is black potassium-bearing shale, the surrounding rocks, and ore layers are mainly carbonated, and the geological structure of the mine is of a simple type.

The article's study area is the phosphorus-bearing rock system of the Sinian era Lower Series Doushantuo Formation (see Figure 1(b)). There are three phosphate formations in the Sujiapo phosphate mine, consisting of three phosphate formations. The roof of the seam is gray-light gray medium-thick laminated dolomite, locally interbedded with thin laminated dolomite of phosphate rock strips, and the main composition of the ore is dolomite (90%–92%) followed by calcite (6%–8%) with a small amount of quartz; the middle layer is mainly dense massive and striped phosphate massive rock; the floor of the seam is black potassium-bearing shale, with plagioclase and ice feldspar (>60%), followed by hydromica, fluorapatite, quartz and pyrite (>30%), in addition, it contains slightly gypsum and muscovite.

According to the engineering geological conditions of the slowly inclined thin ore body, the phosphate mine is currently produced by the room and pillar method, and after years of mining, the underground mining depth has reached 900 m. As mining continues, the better the rock integrity and brittleness, the more obvious the stress concentration in the deep part of the mine, which creates good conditions for the occurrence of rockburst.

2.2. Deep Rockburst Characteristics of Phosphate Mines. The phosphate ore is a colluvial structure ore body, and the ore is loose and easy to deviate. The roof dolomite contains silica and 7% calcite, which is prone to swelling by water absorption, and the phenomenon of roof delamination and blowing is obvious. After mining, the mining area's mine pillar is seriously deformed (see Figure 2(a)), and the stress concentration in the local area will lead to damage to the roadway sidewall and roof (see Figures 2(b) and 2(c)), these phenomena become unfavorable factors for production.

The mine is divided into three rock burst categories: minor, medium, and heavy rock bursts [17]. Minor rockburst occurs in the work face to advance 10 m region on the roof of the clay mass dolomite, there is a weak tearing sound, ejection distance is short, less hazardous; medium rockburst occurs 3 h after blasting, the integrity of the better, more

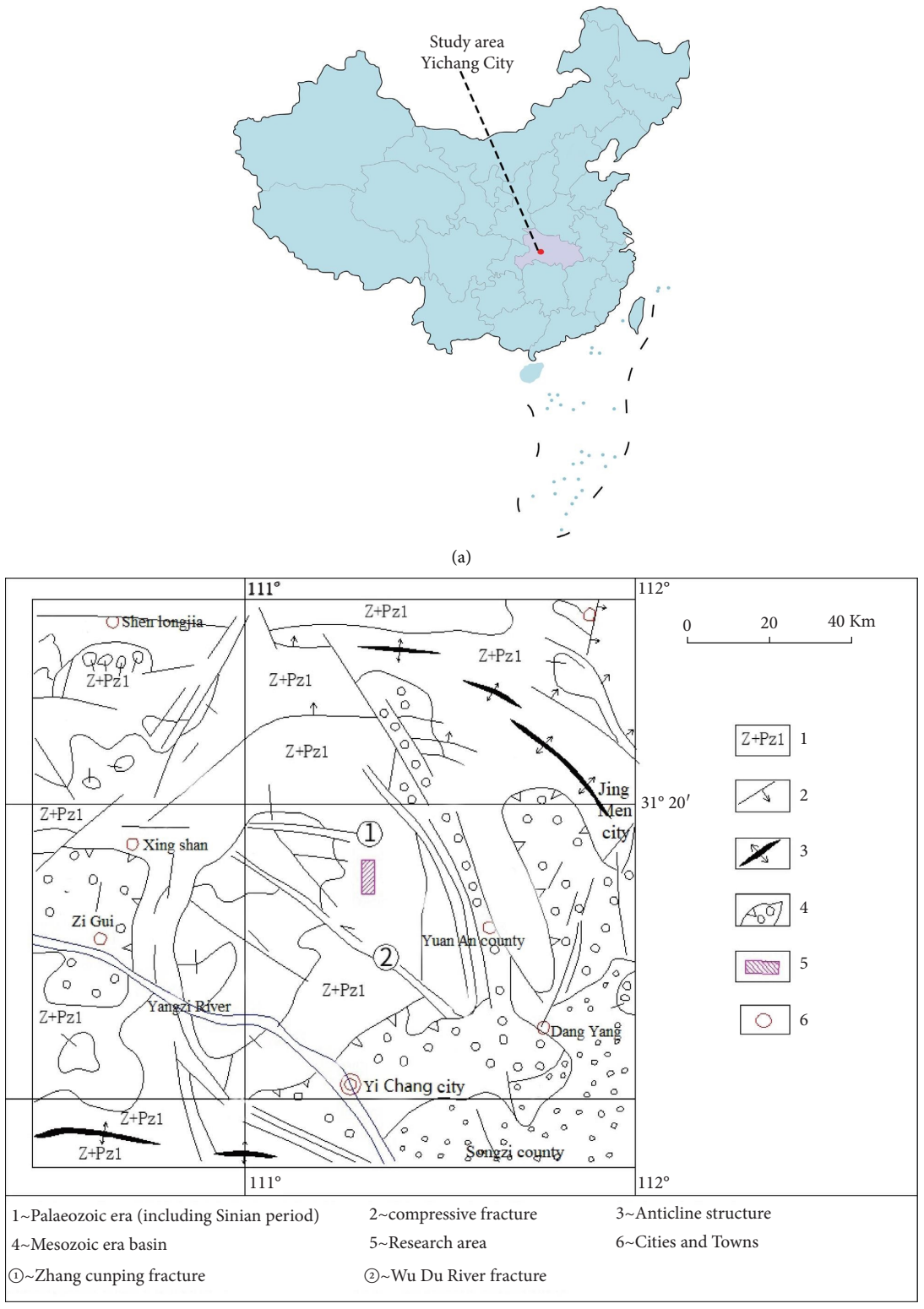

Figure 1: Location and geological structure map of the study area: (a) location map of the study area and (b) geological structure map of the study area.

brittle dolomite roof, there is an obvious fracture sound, the rock to flake ejected more than 2 m, a greater threat to safety; heavy rockburst after blasting, extremely intact, very strong, hard ground pressure is evident in the roof surrounding rock at the sound is huge, serious fracture off the block, flake blast, and ejection distance can reach several meters.

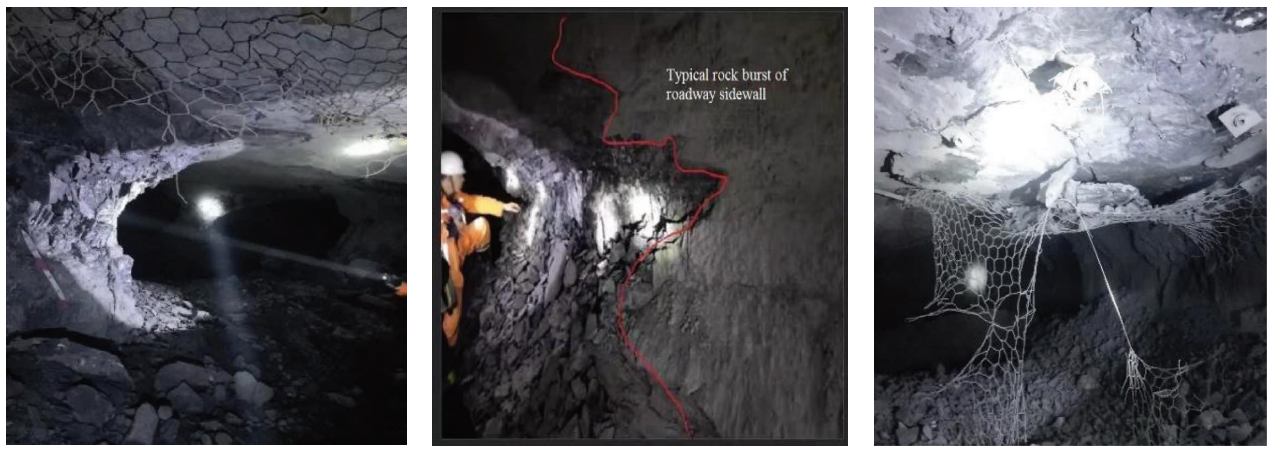

(a) (b) (c)

Figure 2: Schematic diagram of typical location damage: (a) mine pillar deformation; (b) damage to the roadway sidewall; (c) roof damage picture.

3. Rockburst Propensity Analysis

3.1. Determination of Rock Physical Parameters. Three groups of the roof, floor, and ore rocks near the +120 quarry of this phosphate mine were selected for this rock mechanical parameter determination. The sample is directly sampled by a 360° drilling rig on site, and then the collected samples are cut and polished in the laboratory, and finally processed and made into 50 mm × 100 mm cylindrical standard samples (as shown in Figure 3). The splitting method was used to determine the tensile strength using the RTX-1000 high-temperature high-pressure dynamic rock triaxial tester from GCTS, USA (as shown in Figure 4), and the results are shown in Table 1.

3.2. Rockburst Propensity Analysis. Rockburst factors are numerous and complex, single rockburst discrimination is difficult to accurately predict the propensity of deep mining rockburst [18], the discrimination of the propensity of the phosphate mine rockburst from the stress, lithology, and energy considerations, the choice of strength brittleness coefficient method, deformation brittleness coefficient method criterion, Barton criterion, and energy conservation method criterion of the roof, floor, and rockburst propensity of the phosphate mine to make a reasonable judgment The method is based on the following criteria.

3.2.1. Evaluation of Strength Brittleness Factor Method (B Value Method). Studies have shown that brittle rocks have a higher propensity to rock burst, and the brittleness coefficient index is based on the brittle mechanical characteristics of the rock, the uniaxial compressive strength of the rock, and tensile strength ratio B to determine the propensity to rockburst, according to the results of relevant studies, the indicator judgment guidelines are as follows:

$$\begin{cases} B \geq 40, & \text{rockless,} \\ 40 > B \geq 26.7, & \text{weak rockburst,} \\ 26.7 > B \geq 14.5, & \text{medium rockburst,} \\ B < 14.5, & \text{violent rockburst.} \end{cases} \quad (1)$$

3.2.2. Deformation Brittleness Coefficient Method. Rock brittle damage refers to the form of damage in which the rock does not show significant permanent deformation before rupture, the brittleness of the rock is manifested by significant deformation of the strain before and after the peak under uniaxial loading, the deformation brittleness coefficient method is based on the stress-strain curve of the specimen, the total strain, and permanent deformation ε before the peak of the rock, for rockburst propensity evaluation, as shown in the following equation:

$$K_u = \varepsilon/\varepsilon_1 = \frac{\left(\varepsilon_p + \varepsilon_e\right)}{\varepsilon_p}, \quad (2)$$

where ε_p is the plastic deformation; ε_e is the permanent deformation.

The guidelines for the identification of rock bursts are as follows:

$$\begin{cases} \varepsilon/\varepsilon_1 \geq 7, & \text{violent rockburst,} \\ 7 > \varepsilon/\varepsilon_1 \geq 5, & \text{medium rockburst,} \\ 5 > \varepsilon/\varepsilon_1 \geq 3.5, & \text{weak rockburst,} \\ \varepsilon/\varepsilon_1 < 3.5, & \text{rockless.} \end{cases} \quad (3)$$

3.2.3. Barton Criterion. Barton found that after excavation of an underground chamber, stresses around the cavern wall rock are redistributed, resulting in a significant degree of

Figure 3: Sample picture.

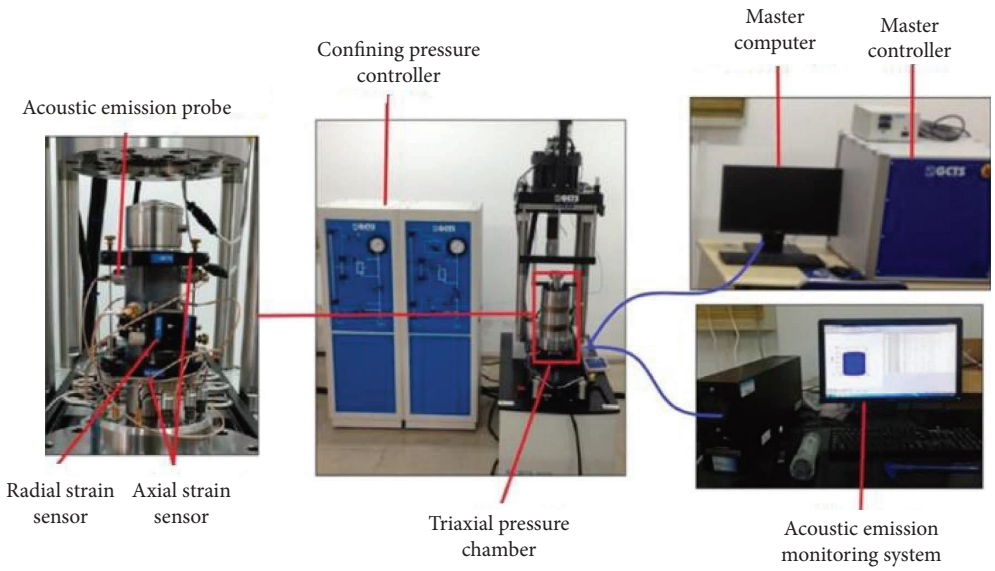

Figure 4: Triaxial test system.

Table 1: Table of results of physical and mechanical determination of rocks.

Location	Number	Density (g/cm^3)	Surrounding pressure (MPa)	Compressive strength (MPa)	Shear strength (MPa)	Poisson's ratio	Cohesive force (MPa)	The angle of internal friction (°)
Ore sample	K-1	3.00	0	19.596	6.6821	0.300	4.42	47
	K-3	3.07	8	37.016	9.8945	0.221		
	K-5	3.00	10	75.098	22.1984	0.286		
Roof	D-2	2.83	0	148.858	22.6338	0.261	9.68	71
	D-5	2.84	8	164.436	26.8031	0.224		
	D-3	2.82	10	188.630	29.4427	0.272		
Floor	d-1	2.75	0	84.835	16.3890	0.32	10.41	64
	d-2	2.77	5	97.933	21.4473	0.23		
	d-5	2.77	10	130.504	27.4853	0.12		

stress concentration in some areas, when the ratio α of σ_c (the uniaxial compressive strength of rock mass) to R_c (the maximum ground stress of rock mass) exceeds a certain range will cause different degrees of rock burst, α is judged by the following guidelines:

$$\begin{cases} \alpha \geq 10, & \text{rockless,} \\ 10 > \alpha \geq 5, & \text{weak rockburst,} \\ 5 > \alpha \geq 2.5, & \text{medium rockburst,} \\ \alpha < 2.5, & \text{violent rockburst.} \end{cases} \quad (4)$$

According to the relevant results, the maximum ground stress R_c is taken as 10.2 MPa in the vertical direction.

3.2.4. Energy Conservation Method Evaluation. According to the law of conservation of energy, the sudden release of energy within the rock causes a rockburst, and the work done by the rock under uniaxial compression is equal to the strain energy stored within the rock, as shown in the following equation:

$$W = \sigma_c \times \varepsilon \times V, \tag{5}$$

where W is the work done by uniaxial compression; ε is the compressive strain of rocks; V is the volume of the rock specimen.

The guidelines for discriminating between rockburst energy indicators are as follows:

$$\begin{aligned} W \geq 39.25J&, \text{ extreme intensity rockburst,} \\ 39.25 > W \geq 19.625&, \text{ violent rockburst,} \\ 19.625 > W \geq 7.85&, \text{ medi um rockburst,} \\ W < 7.85&, \text{ weak rockburst.} \end{aligned} \tag{6}$$

3.3. Results of Rockburst Propensity Evaluation for Each Indicator. By considering several aspects of the mining stress, lithology, and energy, this analysis of rockburst propensity is based on several criteria of rockburst strength brittleness factor criterion, deformation brittleness factor criterion, Barton criterion, and energy method criterion, the rockburst discrimination results of the roof and floor of this phosphate mine, and the mine rock is determined as follows Table 2.

The three rockburst intensity classes obtained using different rockburst propensity evaluation methods differ significantly. On the one hand, due to the influence of rock integrity, there is a slight error in the parameter test results, on the other hand, due to the difference in the factors considered by different evaluation methods, only a certain indicator to consider the results, will inevitably have an impact on the true results. According to the fuzzy mathematics of a bit, the establishment of rock burst propensity judgment matrix, comprehensive consideration of the results of the evaluation indicators for quantitative analysis.

3.4. Fuzzy Mathematical Evaluation of Rockburst Propensity. The fuzzy comprehensive evaluation uses the viewpoint of fuzzy mathematics to establish a fuzzy set of fuzzy objects and fuzzy viewpoints, and the correlation affiliation function distribution theory is used to derive the affiliation function, it will quantitatively analyze the fuzzy set composed of each event. The fuzzy comprehensive evaluation uses fuzzy mathematical methods for the overall evaluation of all events, which has the characteristics of multilevel, multidirectional, and multimeans processing of complex problems [19]. Combined with the results of the evaluation of the four indicators of the rockburst propensity of the Sujiapo phosphate mine, the overall evaluation of the rockburst propensity of this phosphate mine can be made by the method of fuzzy mathematics.

3.4.1. Establishing the Set of Factors Z for Judging the Object. The set of factors for judging the object can be established using the single-indicator rockburst propensity evaluation criteria in the previous section as a set of factors Z. The elements within set Z include rock strength brittleness factor (B), rock deformation brittleness factor (K_u), Barton criterion (α), and energy conservation criterion (W).

$$Z = \{Z_1, Z_2, Z_3, Z_4\} = \{B, K_u, \alpha, W\}. \tag{7}$$

The set of factors judged for each rock sample is shown in Table 3.

3.4.2. Establishment of a Rockburst Propensity Rubric Set U. According to the classification of the different rockburst propensity assessment levels in the previous section, they can be classified as strong rockburst propensity, moderate rockburst propensity, weak rockburst propensity, and no rockburst propensity, then a rockburst propensity rubric set U can be established, namely,

$$U = \{\text{rockless, weak rockburst, medi um rockburst, violent rockburst}\} = \{U_1, U_2, U_3, U_4\}. \tag{8}$$

3.4.3. Determination of Fuzzy Relationship Matrix and Affiliation Function. The fuzzy evaluation matrix $R = \{r_{ij}\}_{m\times n}$ The affiliation degree of each factor determines the final evaluation result, and the method of solving the affiliation function is also particularly important for the overall evaluation result. The affiliation function is determined mainly by binary comparison ranking, fuzzy statistics, empirical analogy, and other methods. Common fuzzy distributions are (half) rectangular distribution, (half) trapezoidal distribution, (half) Gaussian distribution, and other distribution functions. In this paper, according to the engineering situation of rockburst affiliation function distribution is chosen K times parabolic shape distribution [20], the specific solution method is as follows:

Table 2: Table of results of rockburst propensity discrimination.

Rocky sample	Number	B value method		Deformation brittleness criterion		Barton jurisprudence		Energy law jurisprudence	
		σ_c/σ_τ	Inclination	$\varepsilon/\varepsilon_1$	Inclination	σ_c/R_c	Inclination	W	Inclination
Phosphorite	KY-1	14.28	(Violently) strong	4.26	Weak	4.93	Medium	6.54	Not
	KY-4	17.37	Medium	5.84	Medium	5.60	Weak	14.07	Weak
Upper dolomite	D-1	31.70	Weak	7.45	Powerful	8.82	Weak	20.67	Medium
	D-2	57.94	Not	6.67	Medium	16.12	Not	37.82	Medium
Potash-bearing shale	d-1	26.27	Medium	4.72	Weak	9.60	Weak	18.65	Weak
	d-4	28.79	Weak	3.78	Weak	10.52	Not	22.52	Medium

Table 3: Set of factors for each rock sample judging object.

Set Z	Each evaluation factor Z_i set					
	Phosphorite		Dolomite		Shale	
	K-1	K-4	D-1	D-2	d-1	d-4
Z_1 (rock strength brittleness factor B)	14.28	17.37	31.70	57.94	26.27	28.79
Z_2 (rock deformation brittleness factor K_u)	4.26	5.84	7.45	6.67	4.72	3.78
Z_3 (barton criterion α)	4.93	5.60	8.82	16.12	9.60	10.52
Z_4 (energy conservation criterion W)	6.54	14.07	20.67	37.82	18.65	22.52

$$
\begin{aligned}
U_1\colon A_1(x) &= \begin{cases} 1, & x \le a_i, \\ \dfrac{b_i - x_i}{b_i - a_i}, & a_i < x \le b_i, \\ 0, & x > b_i, \end{cases} \\
U_2\colon A_2(x) &= \begin{cases} \dfrac{b_i - a_i}{b_i - x_i}, & x \le a_i, \\ 1, & a_i < x \le b_i, \\ \dfrac{b_i - a_i}{b_i - x_i}, & x > b_i, \end{cases} \\
U_3\colon A_3(x) &= \begin{cases} \dfrac{c_i - b_i}{c_i - x_i}, & x \le b_i, \\ 1, & b_i < x \le c_i, \\ \dfrac{c_i - b_i}{x_i - b_i}, & x > c_i, \end{cases} \\
U_4\colon A_4(x) &= \begin{cases} 0, & x \le b_i, \\ \dfrac{x_i - b_i}{c_i - b_i}, & b_i < x \le c_i, \\ 1, & x > c_i, \end{cases}
\end{aligned} \tag{9}
$$

where A_1, A_2, A_3, and A_4 are the affiliation functions of indicator x_i corresponding to the four rockburst intensity levels; x_i is the ith factor indicator size; a_i, b_i and c_i are the three cut-off values of the i-element corresponding to the rockburst intensity.

(1) Phosphorite subordination function

$$
\begin{aligned}
R_{KY-1} &= \begin{Bmatrix} 0 & 0.52 & 1.00 & 0.98 \\ 0.49 & 1.00 & 0.73 & 0 \\ 0 & 0.98 & 1.00 & 0.03 \\ 1.00 & 0.90 & 0.60 & 0 \end{Bmatrix}, \\
R_{KY-4} &= \begin{Bmatrix} 0 & 0.59 & 1.00 & 0.76 \\ 0 & 0.64 & 1.00 & 0.42 \\ 0.12 & 1.00 & 0.81 & 0 \\ 0.47 & 1.00 & 0.78 & 0 \end{Bmatrix}.
\end{aligned} \tag{10}
$$

(2) Dolomite affiliation function

$$
\begin{aligned}
R_{D-1} &= \begin{Bmatrix} 1.00 & 0.38 & 0.71 & 0 \\ 0 & 0.38 & 0.82 & 1.00 \\ 0.66 & 1.00 & 0.47 & 0 \\ 0 & 0.92 & 1.00 & 0.05 \end{Bmatrix}, \\
R_{D-2} &= \begin{Bmatrix} 1.00 & 0.43 & 0.28 & 0 \\ 0 & 0.47 & 1.00 & 0.84 \\ 1.00 & 0.45 & 0.18 & 0 \\ 0 & 0.39 & 1.00 & 0.93 \end{Bmatrix}.
\end{aligned} \tag{11}
$$

(3) Shale affiliation function

$$R_{d-1} = \begin{Bmatrix} 0 & 0.03 & 1.00 & 0.04 \\ 0.19 & 1.00 & 0.88 & 0 \\ 0.92 & 1.00 & 0.35 & 0 \\ 0.08 & 1.00 & 0.95 & 0 \end{Bmatrix},$$
$$R_{d-2} = \begin{Bmatrix} 0.16 & 1.00 & 0.85 & 0 \\ 0.81 & 1.00 & 0.62 & 0 \\ 1.00 & 0.91 & 0.88 & 0 \\ 0 & 0.80 & 1.00 & 0.15 \end{Bmatrix}. \quad (12)$$

3.4.4. Weighting of Propensity Indicator Factors. According to the importance of the four evaluation indicators of rockburst propensity, each indicator is assigned a weight to obtain the weight set of influence factors. The greater the effect of the indicator factors on the propensity to rockburst, the closer the assigned weight value is to 1, and the sum of the weight values of the four indicators is 1.

There are many methods to determine the weight value, such as the commonly used: AHP hierarchical analysis method, the superior order diagram method, the CRITIC method, the entropy weight method, etc. The various methods differ in terms of data size information, volatility and interrelationships. In this paper, by searching various weighting methods and combining them with the expert scoring system, we use the expert scoring method for the weighting of indicator factors, and the results of the weighting of each indicator factor are as follows.

$$A = \left(a_{1,}a_{2,}a_{3,}a_{4,}\right) = (0.20, 0.30, 0.20, 0.30). \quad (13)$$

3.4.5. Comprehensive Evaluation of Rockburst Propensity. Substituting the set of indicator factor weights and the intensity level affiliation fuzzy function into equation $F = A * R = (y_1, y_2, y_3, y_4)$ gives.

(1) Phosphorite maximum probability criterion

$$F_{k-1} = A \bullet R = (0.20, 0.30, 0.20, 0.30) \times \begin{bmatrix} 0 & 0.52 & 1.00 & 0.98 \\ 0.49 & 1.00 & 0.73 & 0 \\ 0 & 0.98 & 1.00 & 0.03 \\ 1.00 & 0.90 & 0.60 & 0 \end{bmatrix} = (0.447, 0.87, 0.799, 0.202),$$
$$F_{K-4} = A \bullet R = (0.20, 0.30, 0.20, 0.30) \times \begin{bmatrix} 0 & 0.59 & 1.00 & 0.76 \\ 0 & 0.64 & 1.00 & 0.42 \\ 0.12 & 1.00 & 0.81 & 0 \\ 0.47 & 1.00 & 0.78 & 0 \end{bmatrix} = (0.165, 0.81, 0.887, 0.278). \quad (14)$$

Through the comprehensive evaluation of the rockburst tendency of phosphate rock, the maximum affiliation of KY-1 is 0.87, corresponding to the U_2 level, and the maximum affiliation of KY-4 is 0.887, corresponding to the U_3 level, according to the principle of maximum affiliation, the maximum affiliation of phosphate block rock takes the value of 0.887, and the comprehensive evaluation result is medium rockburst tendency.

(2) Dolomite rock maximum probable criterion

$$F_{D-1} = A \bullet R = (0.20, 0.30, 0.20, 0.30) \times \begin{bmatrix} 1.00 & 0.38 & 0.71 & 0 \\ 0 & 0.38 & 0.82 & 1.00 \\ 0.66 & 1.00 & 0.47 & 0 \\ 0 & 0.92 & 1.00 & 0.05 \end{bmatrix} = (0.322, 0.666, 0.782, 0.315),$$
$$F_{D-2} = A \bullet R = (0.20, 0.30, 0.20, 0.30) \times \begin{bmatrix} 1.00 & 0.43 & 0.28 & 0 \\ 0 & 0.47 & 1.00 & 0.84 \\ 1.00 & 0.45 & 0.18 & 0 \\ 0 & 0.39 & 1.00 & 0.93 \end{bmatrix} = (0.40, 0.436, 0.692, 0.531). \quad (15)$$

Through the comprehensive evaluation of the dolomite rockburst propensity, the maximum affiliation of D-1 is 0.782, corresponding to the U_3 level, and the maximum affiliation of D-2 is 0.692,

corresponding to the U_3 level. According to the principle of maximum affiliation, the maximum affiliation of dolomite takes the value of 0.782, and the comprehensive evaluation result is medium rockburst propensity.

(3) Maximum Possible Judgment for Shale Rocks

$$\begin{aligned} F_{d-1} &= A \bullet R = (0.20, 0.30, 0.20, 0.30) \times \begin{bmatrix} 0 & 0.03 & 1.00 & 0.04 \\ 0.19 & 1.00 & 0.88 & 0 \\ 0.92 & 1.00 & 0.35 & 0 \\ 0.08 & 1.00 & 0.95 & 0 \end{bmatrix} = (0.265, 0.806, 0.819, 0.008), F_{d-4} \\ &= A \bullet R = (0.20, 0.30, 0.20, 0.30) \times \begin{bmatrix} 0.16 & 1.00 & 0.85 & 0 \\ 0.81 & 1.00 & 0.62 & 0 \\ 1.00 & 0.91 & 0.88 & 0 \\ 0 & 0.80 & 1.00 & 0.15 \end{bmatrix} = (0.475, 0.922, 0.832, 0.045). \end{aligned} \tag{16}$$

Through the comprehensive evaluation of the shale rockburst propensity, the maximum affiliation of d-1 is 0.819, corresponding to the U_3 level, and the maximum affiliation of d-4 is 0.922, corresponding to the U_2 level. According to the principle of maximum affiliation, the maximum affiliation of shale takes the value of 0.922, and the comprehensive evaluation results in weak rockburst propensity.

4. Analysis of the Microscopic Mechanism of Rockburst Damage

The extension and damage of internal joint fractures in rocks under the action of external forces are related to factors such as rock microstructure and degree of crystallization, and the microstructure of rockburst debris can effectively reflect the force damage characteristics and mechanical properties of rocks during rockburst [21], and dynamically reveal the mechanistic characteristics of rockburst fracture generation, an extension until rupture, and the mineral composition of rocks is one of the important factors determining the degree of rock damage [22]. Therefore, microstructure analysis is of great significance for the study of the rockburst fracture mechanism.

4.1. Rockburst Debris Microscopic Morphology Analysis. The JSM-500LV scanning electron microscope was selected to analyze the microscopic morphological characteristics and elemental composition of the rock samples, and two pieces each of rockburst roof and phosphate rock were selected in the typical rockburst area +120 South Q2 quarry (burial depth about 900m) to analyze the microscopic morphological characteristics, damage form, and micromechanics of the debris (see Figures 5 and 6).

The macroscopic composition of the clastic surface of the roof sample is composed of dolomite cemented with other minerals, and fissures exist on the surface of the sample. The overall structure of the sample is relatively dense, but there are several small hollow pores on the surface, as observed by magnification to 1 μm. The fracture mechanism is that after the initial fracture of the rock along the crystal boundary, with the propagation of stress waves, a large number of stress waves intersect and pass through, reflecting superposition, and stretching and staggering by the elastic energy of the rockburst lead to the brittle fracture of the step-like fracture, and the fracture expands to form a plate and laminated structure.

The mineral rock grains in phosphorite are surrounded by other mineral grains, there are a large number of intermittent pores between the grains, the surface roughness of the grains is high and three-dimensional, and the grains and pores are randomly and disorderly distributed. In Figure 5(c), it can be seen that the rock debris accumulation of the rock sample, the main breaking style, and fracture character is lamellar damage, and there is a clear fracture in the rock sample, the fracture mechanism is mainly in the form of shearing and pulling Under external loading, stress waves propagating between the particles will exist in a pore compression process, as the stress waves interact and superimpose between the grain surfaces, small fissures penetrate to form a large number of pores and fissures, and cracks along the void expand rapidly and complex shape, until the expansion penetration, tearing, mineral particles flake and separate under shear, and the strength of the rock decreases.

In summary, it can be seen that the roof dolomite is a mainly brittle fracture with step-like fractures and slab-like fractures. The phosphorite block is mainly shear tearing along the crystal, and the fracture is a rough and disorder-like fracture. The energy consumption required for brittle fracture of the roof dolomite is greater than that required for fracture along the crystal of the phosphorite block, but the energy storage performance of the dolomite is much greater than that of the phosphorite block, so the rockburst impact is also greater.

4.2. Rock Acoustic Emission 3D Imaging Analysis. This acoustic emission mainly studies the internal crack expansion process of the rock under triaxial compressive loading

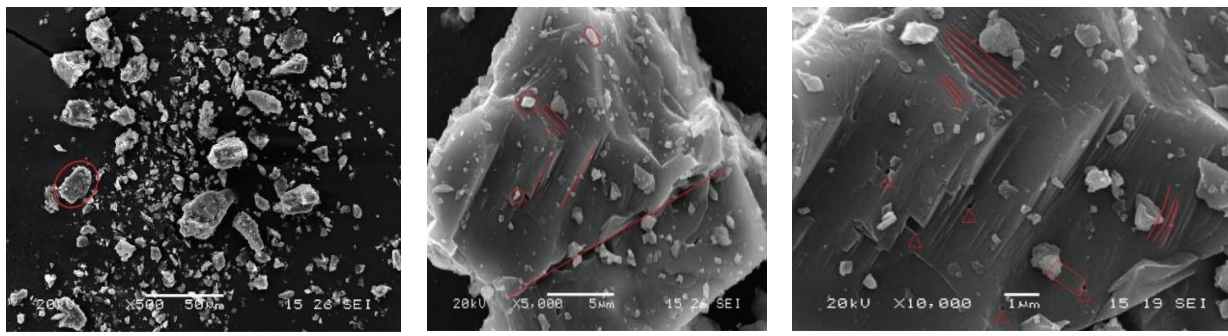

(a) (b) (c)

Figure 5: Microscopic morphology of dolomite roof: (a) 50 μm SEM observation chart; (b) 5 μm SEM observation chart; (c) 1 μm SEM observation chart.

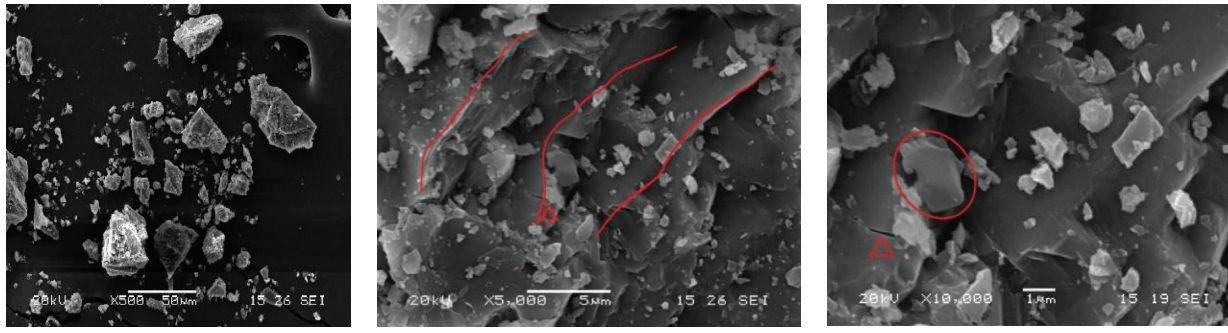

(a) (b) (c)

Figure 6: Microscopic morphology of phosphorite masses: (a) 50 μm SEM observation chart; (b) 5 μm SEM observation chart; (c) 1 μm SEM observation chart.

of the roof and floor ore rocks, analyzes the crack generation and expansion direction of the rock specimen, predicts the rock rupture surface, and further strengthens the research on the rockburst mechanism. Figure 7 to phosphorite specimens as an example to analyze the process of specimen acoustic emission changes under triaxial loading (10 MPa).

From Figure 7 phosphate block rock triaxial load acoustic emission images can be seen in the specimen acoustic emission images broken points sporadically distributed in various parts of the specimen (as shown in Figure 7(a)), but no obvious fractures, at this time the energy is in a slow growth phase; As Yang et al. [23] and Li et al. [24] said with the increase in axial load, increasing number of signals released, acoustic emission images show that the broken points gradually to the right half of the specimen concentration (Figures 7(b) and 7(c)), acoustic emission activity is intense, the number of events increased sharply, the specimen internal broken points gradually to with the continuous loading of the specimen, the acoustic emission activity inside the sample continues to change, the small fragmentation inside the sample increases, the fracture in the right half gradually extends, and develops to the late stage of loading due to the change of the internal structure of the rock, the energy stored inside the rock is released in a large amount in a short period of time, resulting in an obvious splitting damage of the specimen (Figure 7(d)), until the specimen loses load-bearing capacity, the specimen is splitting tensile damage. Phosphor block rock is a medium rock explosion tendency.

4.3. Analysis of the Mechanism of Action of Rock Microcomponents. Rock minerals are generally mineral assemblages formed by the chemistry of multiple elements, and the strength and mechanical properties of rocks are not only related to their microstructure and the adsorption form of colloids, but also the chemical composition of minerals, the arrangement of molecular chemical bonds and other properties lead to the differences in mechanical properties between rocks, i.e., the differences in rockburst mechanical properties between the storage and sudden release of elastic strain energy of rocks under external forces. The mineral element composition of the rock is one of the important factors in determining its damage characteristics, and in this case, the roof near the +120 quarry was selected for scanning electron microscopy and EDS energy spectroscopy analysis with the rockburst debris of the mine rock.

From the scanning electron microscope EDS pattern of the above rock sample (Figures 8 and 9), the composition analysis table of the rock sample (Tables 4 and 5, Wt and At in the table indicates the weight percentage and atomic number percentage of elements, respectively), it can be seen

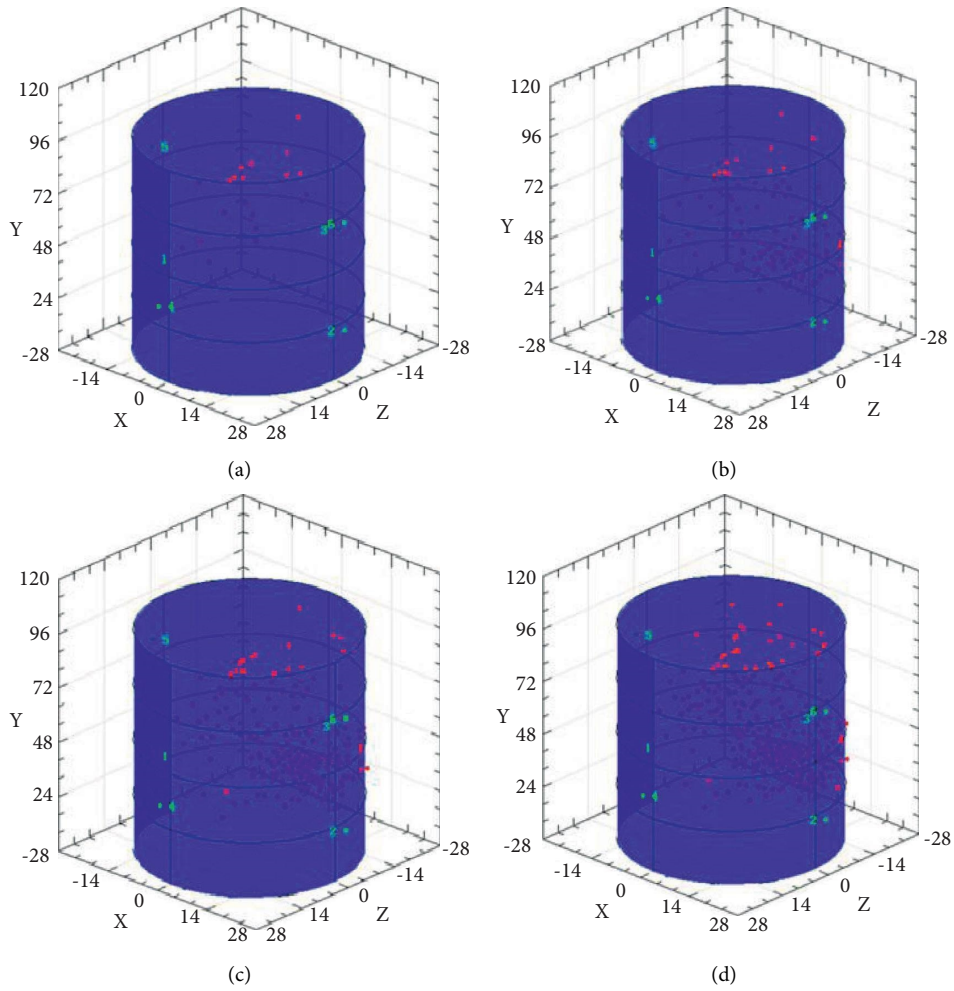

Figure 7: Acoustic emission image of the rock sample.

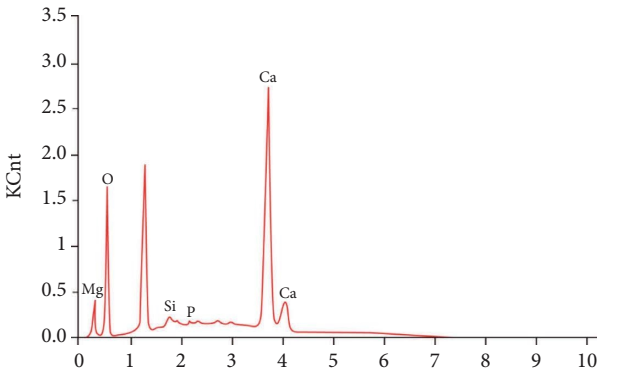

Figure 8: Electron microscopy scanning EDS profile of the roof of the upper dolomite.

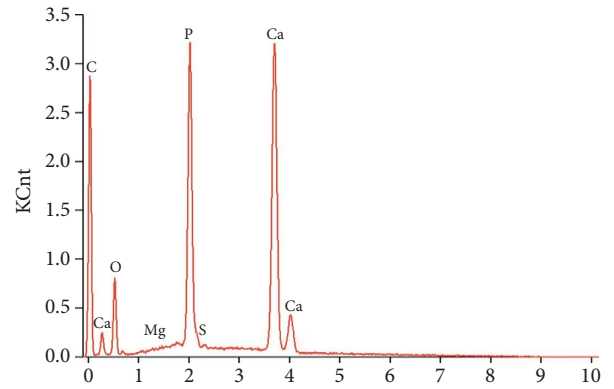

Figure 9: Electron microscopy scanning EDS profile of the phosphorite block.

that the roof of the upper dolomite contains five elements, O, Si, P, Mg and Ca, and the main chemical composition is CaO, and a small amount of SiO_2 exists, and the roof has good integrity, dense grains, and high crystallinity, indicating that The high cohesion between the molecules of the roof material, high elastic modulus, high strength, and the ability of the roof rock sample to store elastic strain energy under the external load. And the obvious presence of siliceous dolomite can be seen in some of the downhole roof rockburst areas, and in the roof area with high SiO_2 content, the siliceous dolomite absorbs water and is easy to delaminate. In addition, The presence of C in the assay results may be due to surface metallization during on-site sampling, this part is explained in the analysis section. Zhao et al. [25]

Table 4: Elemental composition analysis of the upper dolomite roof.

Elemental	Wt%	At%
O	65.78	82.70
Si	0.54	0.39
P	0.10	0.06
Mg	0.72	0.42
Ca	32.86	16.43

Table 5: Analysis of the elemental composition of phosphate block rock.

Elemental	Wt%	At%
O	12.47	24.00
P	21.56	21.44
Ca	63.49	48.79
C	2.10	5.38
S	0.33	0.32
Mg	0.06	0.07

analyzed the elemental composition of sandstones in the mine area and concluded that differences in the mineral composition of the ore bodies for the same study area also caused differences in material destruction characteristics. Therefore, from Table 5, it can be seen that the phosphate massive rocks not only contain O, Ca, Mg, and P four elements, but also contain a small amount of S, indicating that the chemical composition of phosphorite rock samples is more complex, some compounds, and useful ore body cementation to form ore, the shape, and distribution of the particles are not uniformly arranged, and S elements in the crystal boundary easy to deviated, desolvation, the degree of crystallization is poor, cementation of amorphous minerals due to particle grain crystal fine The amorphous minerals formed by cementation have low crystallinity, low cohesion, low elastic modulus, low strength, and easy deformation [25].

From the above findings, it can be seen that the roof dolomite is more crystalline than the phosphate block rock, has high elastic modulus, and high strength, under the action of external loading, the roof dolomite stores more elastic strain energy, deformation damage consumes less energy, the energy released to the outside after damage is large, prone to brittle damage, high propensity to rockburst. Therefore, with the less elemental species of the rock, its internal particle arrangement is more uniformly distributed, high degree of crystallization, high strength, and high elastic modulus, and the external force is more likely to occur under the action of rockburst.

5. Conclusion

(1) Rockburst propensity to discriminate, should be considered from the stress, lithology, energy, and burial depth of multiple factors, a single indicator of the evaluation results often differs, with certain limitations, using multiple evaluation methods to comprehensively judge rockburst propensity is the easiest to obtain the required parameters through the test, and the results are reliable. The study shows that dolomite and phosphorite in the study area are moderate rockburst, and shale has a weak rockburst tendency.

(2) Rock acoustic emission activity corresponds to each stage of the rock damage process, reflecting the whole process of rock crack extension and expansion. The pattern of acoustic emission events correlates with rock lithology, and the frequency of acoustic emission activity directly reflects the degree of rockburst energy accumulation.

(3) It is known from the analysis of scanning electron microscopy and EDS profile that the roof dolomite has fewer constituent elements than the phosphoric block rock, has a high degree of crystallization, has a high elastic modulus, stores more strain energy under external loading, consumes less energy for deformation damage, and is prone to rockburst. The ability of the rock to store and release elastic strain energy is related to the tectonics and adsorption of mineral grains, with dolomite being brittle fracture and phosphorite block rock being dominated by fracture along the crystal.

Data Availability

The data used to support the findings of this study are included within the article.

Conflicts of Interest

The author (s) declare (s) that there are no conflicts of interest regarding the publication of this paper.

Acknowledgments

The authors would like to thank the reviewers for improving this manuscript. This research was supported by the National Natural Science Foundation of China (No. 52174086) and the Graduate Education Innovation Fund (No. CX2021477).

References

[1] X. Li, S. Chen, S. Wang et al., "Study on in situ stress distribution law of the deep mine taking Linyi Mining area as an example," *Advances in Materials Science and Engineering*, vol. 2021, no. 4, Article ID 5594181, 11 pages, 2021.

[2] A. Mazaira and P. Konicek, "Intense rockburst impacts in deep underground construction and their prevention," *Canadian Geotechnical Journal*, vol. 52, no. 10, pp. 1426–1439, 2015.

[3] S. Wang, X Li, Q. L. Qin, and Q. Z. Qin, "Study on surrounding rock control and support stability of Ultra-large height mining face," *Energies*, vol. 15, no. 18, p. 6811, 2022.

[4] S. Lv, *Research on the Mechanism and Application of Rockburst in Underground Engineering under High Ground Stress*, Graduate School of Chinese Academy of Sciences (Wuhan Institute of Geotechnics), Wu Han, China, 2009.

[5] W. B. Yan, T. T. Wang, and T. Liu, "Mechanism of rockburst occurrence in deep mine area of factory dam lead-zinc mine and classification of the danger zone," *Mining Research and Development*, vol. 38, no. 5, pp. 50–55, 2018.

[6] M. F. Cai, D. Yi, and Q. F. Guo, "Research on rockburst prediction based on ground stress field measurements and mining disturbance energy accumulation theory," *Journal of Rock Mechanics and Engineering*, vol. 10, pp. 1973–1980, 2013.

[7] A. Zubelewicz and Z. Mroz, "Numerical simulation of rock burst processes treated as problems of dynamic instability," *Rock Mechanics and Rock Engineering*, vol. 16, no. 4, pp. 253–274, 1983.

[8] J. D. Li, L. Guan, L. Q. Han, and C. Y. Miao, "Analysis of micro-crack characteristics from rockburst failure of basalt in Baijiao coal Mine content," *Journal of China Coal Society*, vol. 39, no. 2, pp. 307–314, 2013.

[9] M. Q. Lin, L. Zhang, X. Q. Liu, Y. Y. Xia, D. J. Zhang, and Y. L. Peng, "Microscopic analysis of rockburst failure on specimens under gradient stress," *Rock and Soil Mechanics*, vol. 41, no. 9, pp. 2984–2992, 2019.

[10] B. Huang, S. L. Li, and Z. P. Gao, "Comprehensive evaluation of rockburst in deep shaft large-scale mining of Da Hongshan iron ore mine," *Metal Mining*, vol. 45, no. 5, pp. 19–25, 2016.

[11] Y. Lin, S. L. Du, and C. D. Ma, "Fuzzy comprehensive evaluation of rockburst propensity for deep mining in Maluping mine," *Metal Mining*, vol. 39, no. 4, pp. 10–14, 2010.

[12] M. L. Yuan, K. P. Hou, and H. F. Sun, "Study on prediction of rockburst propensity of a deep shaft enclosure," *Nonferrous Metals*, vol. 73, no. 5, pp. 69–74, 2021.

[13] X. B. Yang, Y. Y. Pei, and H. M. Cheng, "Rockburst intensity level prediction method based on SOFM neural network model," *Journal of Rock Mechanics and Engineering*, vol. 40, no. S1, pp. 2708–2715, 2021.

[14] W. W. Jiang, Z. H. Su, and X. X. Chen, "Rock stability prediction model based on microseismic monitoring," *Mining Research and Development*, vol. 36, no. 11, pp. 41–44, 2016.

[15] X. Y. Liu and H. Y. Ji, "Research on rockburst prediction based on the AdaBoost-BAS-SVM model," *Metal Mining*, vol. 50, no. 10, pp. 28–34, 2021.

[16] H. Zhou, Y Zhang, B. Liu et al., "Research on residual shear strength of surrounding rock base on elastic-plastic softening model," *E3S Web of Conferences*, vol. 198, p. 01034, 2020.

[17] X. Feng, Y. Xiao, and G. Feng, "Study on the development process of rockburst," *Chinese Journal of Rock Mechanics and Engineering*, vol. 38, no. 4, pp. 649–673, 2019.

[18] J. Yang and L. J. Wang, "Experimental study on acoustic emission of rockburst mechanism," *Journal of Rock Mechanics and Engineering*, vol. 20, pp. 198–204, 2005.

[19] W. Z. Zhang, W. Q. Wang, and Y. L. Peng, "AHP-FUZZY-based optimization of the room-and-pillar method for the exit of section IV of Wawu phosphate mine," *Metal Mining*, vol. 51, no. 9, pp. 18–24, 2022.

[20] X. Wen, C. Huang, and M. Tan, "Prediction of rockburst propensity of deep rock masses in Ashlee copper mine based on the fuzzy mathematical method," *Nonferrous Metals*, vol. 73, no. 4, pp. 72–79, 2021.

[21] Z. Song, "Experimental Experimental Study on the Characteristics of Acoustic Emission Source of Rock under Uniaxial Compressiontudy on the characteristics of acoustic emission source of rock under uniaxial compression," *IOP Conference Series: Earth and Environmental Science*, vol. 791, no. 1, Article ID 012003, 2021.

[22] W. Z. Chen, S. P. Lv, and X. H. Guo, "Study on unloading pressure test and rockburst mechanism of brittle rock," *Journal of Geotechnical Engineering*, vol. 32, no. 6, pp. 963–996, 2010.

[23] D. Yang, J. Hu, S. Ma, and PP. Zeng, "Analysis of dynamic fracture of granite after uniaxial recompression predamaged by high confining pressure cyclic loading based on acoustic emission," *Engineering Fracture Mechanics*, vol. 266, no. 9, Article ID 108414, 2022.

[24] L. R. Li, J H Deng, L Zheng, J. F. H. Liu, L. Zheng, and J. F. Liu, "Dominant Dominant Frequency Characteristics of Acoustic Emissions in White Marble During Direct Tensile Testsrequency characteristics of acoustic emissions in white marble during direct tensile tests," *Rock Mechanics and Rock Engineering*, vol. 50, no. 5, pp. 1337–1346, 2017.

[25] K. Zhao, H. Zhao, and Q. Jia, "An analysis of rockburst fracture micromorphology and study of its mechanism," *Explosion and Shock Waves*, vol. 35, no. 6, pp. 913–918, 2015.